



Originally published as:

Yoon, J.-S., Zang, A., Stephansson, O., Zimmermann, G. (2016): Modelling of Fluid-injection-induced Fault Reactivation Using a 2D Discrete Element Based Hydro-mechanical Coupled Dynamic Simulator. - *Energy Procedia*, 97, pp. 454–461.

DOI: <http://doi.org/10.1016/j.egypro.2016.10.049>



European Geosciences Union General Assembly 2016, EGU
Division Energy, Resources & Environment, ERE

Modelling of fluid-injection-induced fault reactivation using a 2D discrete element based hydro-mechanical coupled dynamic simulator

Jeoung Seok Yoon^{a,*}, Arno Zang^a, Ove Stephansson^a, Günter Zimmermann^b

^aSection 2.6 Seismic Hazard and Stress Field, Helmholtz Centre Potsdam GFZ German Research Centre for Geosciences, Telegrafenberg, Potsdam 14473, Germany

^bSection 6.2 Geothermal Energy Systems, Helmholtz Centre Potsdam GFZ German Research Centre for Geosciences, Telegrafenberg, Potsdam 14473, Germany

Abstract

Fluid-injection-induced seismicity often accompanies reactivation of natural fault systems which has become a major environmental problem in the fields of development of Enhanced Geothermal Systems, extraction of hydrocarbon in shale gas reservoirs, and waste water disposal. We present a numerical modelling and investigate how the seismicity induced by nearby high-rate fluid injection evolves depending on the effect of permeability contrast between the fault systems and the reservoir rock. Modelled magnitude of induced seismicity tends to be higher with presence of less permeable fault system than the reservoir rock.

© 2016 The Authors. Published by Elsevier Ltd. This is an open access article under the CC BY-NC-ND license (<http://creativecommons.org/licenses/by-nc-nd/4.0/>).

Peer-review under responsibility of the organizing committee of the General Assembly of the European Geosciences Union (EGU)

Keywords: Fluid injection; Induced Seismicity; Fault reactivation; Seismic hazard

* Corresponding author. Tel.: +49-331-288-1716; fax: -49-331-288-1127.
E-mail address: jsyoon@gfz-potsdam.de

1. Introduction

Fluid-injection-induced seismicity often accompanies reactivation of natural fault systems. This issue has become a major environmental problem in the fields of development of Enhanced Geothermal Systems [1], extraction of hydrocarbon in shale gas reservoirs, and waste water disposal [2]. In particular, several damaging earthquakes have been reported in the USA in the areas of high-rate massive amount of waste water injection mostly with natural fault systems. One recent seismic event occurred in 2013 near Azle, Texas where a series of earthquakes began along a mapped ancient fault system [3]. These examples demonstrate that the presence of natural fault systems has significant impact to the environment in the development of energy systems and emphasize the necessity for better understanding of the physical processes that are hydro-mechanical-thermal-(chemical) and even dynamically coupled. In this context, we present a numerical modelling and investigate how seismicity induced by nearby high-rate fluid injection evolves under the presence of fault systems that are in a near-critical stress state. Furthermore, we investigate the effect of permeability contrast between fault systems and reservoir rock mass on seismic responses in terms of induced seismic magnitudes and stress drop and we provide geomechanical interpretation to the results by looking closely into the hydro-mechanical and dynamically coupled processes.

2. Modelling tool and description of the model

As a modelling tool, we present, 2D discrete element based hydro-mechanical coupled dynamic simulator. The simulator is based on commercial software called Particle Flow Code 2D, where the algorithms for fluid flow modelling and seismicity computing are additionally implemented by FISH programming. Details of the modelling method can be found in [4].

A reservoir model is constructed and shown in Figure 1 which represents a 10 meter thick horizontal layer at depth and subjected to maximum and minimum horizontal stresses. An inclined fault zone is modelled as a combination of damage zone and core fractures. The damage zone is represented by smaller particles and bonded with stiffness and strength lower than those in the host rock mass (Table 1). This fault zone structure resembles what is commonly observed in the field at different spatial scales in all kinds of lithologies (siliciclastic or carbonate geological settings). The damage zone is 100 m wide and the fault core is represented by the smooth joint model of PFC2D [5] of which the properties are listed in Table 1. Hydraulic behavior of the fault zone is modelled differently from the host reservoir rock mass by assigning different normal stress vs. hydraulic aperture relation (assumed) to the contacts that are in the damage zone and the host rock mass as shown in Figure 2. Distribution of the permeability at the flow channels in the damage zone and in the host rock mass are shown in Figure 3 to mimic high permeability fault (fluid conduit) and low permeability fault zones (fluid barrier), and named as high-k-FZ-model and low-k-FZ-model, respectively.

Table 1. List of model parameters.

Particle and Parallel bond model property	Host rock mass	Fault zone
Particle density [kg/m ³]	2630	2630
Particle elastic modulus [GPa]	60	40
Particle friction coefficient [-]	0.9	0.5
Bond tensile and cohesion strength [MPa]	9, 25	2, 5
Bond friction angle [Deg]	53	30
Smooth joint model property	Rock fracture	Fault core fracture
Normal and shear stiffness [GPa/m]	60, 5	30, 2
Friction coefficient [-]	0.9	0.5
Tensile and cohesive strength [MPa]	2, 5	0.1, 0.5
Friction and dilation angles [Deg]	50, 3	30, 3

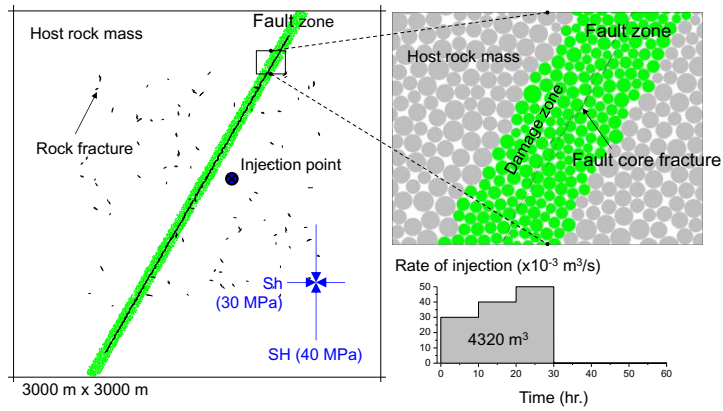


Fig. 1. Reservoir model with inclined fault zone (green) for fluid injection modelling.

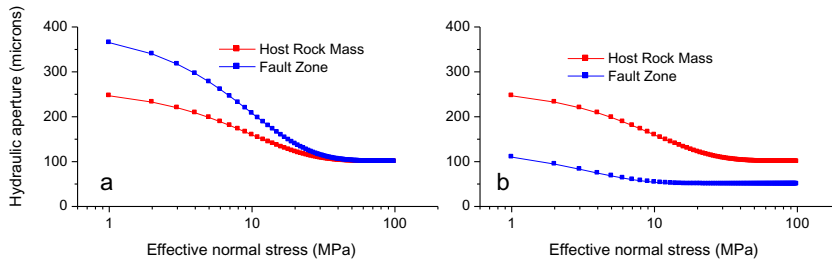


Fig. 2. Relations between hydraulic apertures and effective normal stress of the particle contacts in the host rock mass and in the fault zone for the (a) high-k-FZ and (b) low-k-FZ-models.

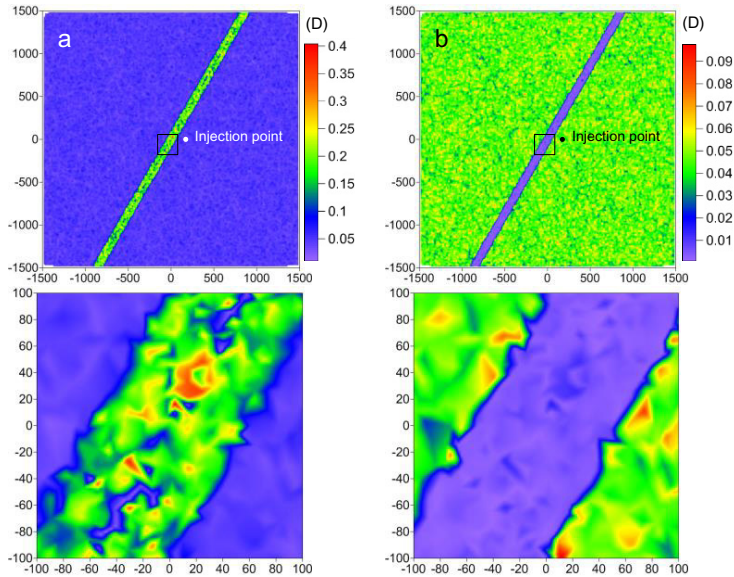


Fig. 3. Permeability contrast between the host rock mass and the fault zone in the (a) high-k-FZ and in (b) low-k-FZ-models.

3. Analysis of fluid-injection-induced seismic events and fault slip

Fluid injection with changing rates over time (0.3, 0.4 and 0.5 m³/s maintained for 10 hours for each rate step) is applied at 200 m distance from the fault zone (see Fig.1). Figure 4 shows temporal and spatial distributions of the induced seismic events, modelled in (a) high-k-FZ-model and in (b) low-k-FZ-model. The symbol size represents the magnitude of stress drops (in MPa) of the events and they are coloured according to their time of occurrence. Those early and late events are in red and in green, respectively. Stress drop ($\Delta\sigma$) is calculated using [6]:

$$\Delta\sigma = \frac{7M_0}{16R^3} \tag{1}$$

where, M_0 is seismic moment (Nm) and R is the source radius (m)

The figure for the high-k-FZ-model demonstrates that the induced seismic events are mostly distributed within and evolve along the fault zone, and except a few, most of the events are characterized by relatively low stress drops (average 0.04 MPa). On the other hand, seismic events evolve in low-permeable fault zone are characterized by higher stress drops (average 0.08 MPa).

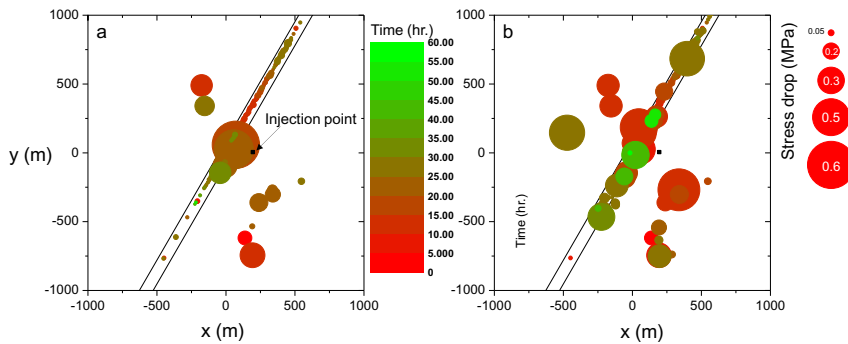


Fig. 4. Temporal and spatial distributions of the induced seismic events in the (a) high-k-FZ and in (b) low-k-FZ-models. Black dot in the middle represents the location of fluid injection point.

Temporal development of the fault core slip is estimated by averaging the shear displacement of the fault core modelled by the smooth joints. In this analysis, slip of the fault core is monitored every hour and the seismic moments (M_0) and the moment magnitude (M_w) of the fault core are calculated using:

$$M_0 = GAd \tag{2}$$

$$M_w = \frac{2}{3} \log(M_0) - 6 \tag{3}$$

where, A is the fault area (m²), G is shear modulus (30 GPa), and d is the average slip.

Figure 5 shows temporal evolution of the seismic magnitude (red) associated with fault core slip induced by fluid injection in the (a) high-k-FZ and in (b) low-k-FZ-models, plotted together with the magnitudes of those seismic events (black). The results demonstrate that the seismic magnitudes associated with the fault core slip (red) are generally larger than those induced events (black), and tend to increase with increasing temporal density of the seismic events occurred in the fault zone. Two models show very different results. The magnitude associated with fault core slip in the low-k-FZ-model reaches M3 (Fig. 5b), whereas it is less than M2 in the high-k-FZ-model (Fig. 5a).

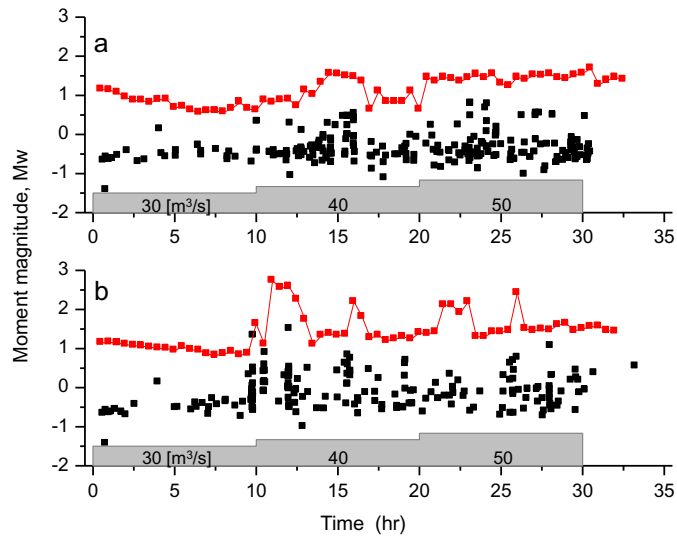


Fig. 5. Temporal change in the magnitudes of the induced seismic events (black) evolving in the fault zone and the seismic magnitude associated with average slip of the fault core in the (a) high-k-FZ and in (b) low-k-FZ-models.

In order to explain this difference, we plotted in Figure 6 the fluid pressure distribution at different times during injection in the (a) high-k-FZ and in (b) low-k-FZ-models. In the high-k-FZ-model, the fluid can easily migrate into the fault zone and follow the fault zone relatively faster than in the host rock mass. As fluid migrates along the fault zone, the fluid lowers the effective normal stress acting on the fault core fracture and leads to shear failure, which follows the theory of effective stress and Mohr-Coulomb failure. However, in the low-k-FZ-model, the injected fluid cannot fully migrate into the fault zone due to the low permeability barrier. Instead it migrates along the interface between the host rock mass and the fault zone. As a result, a large zone of high fluid pressure is build up at one side of the fault zone, which brings the fault zone to a state of higher stress.

Due to the processes described above, the seismic events generated in the less permeable fault zone are larger than those in the high-k-FZ-model in terms of numbers, magnitude and stress drops. We visualize this process in Figure 7 where the area around the injection point and near the fault zone is enlarged to see the fluid migration, fluid pressure distribution, bond breakages and induced seismic events. Fluid pressure is shown in blue where the symbol size represents the pressure magnitude. Fluid flow at the flow channels is shown in cyan where the thickness of the symbol represents the volume of flow at the time when the snapshots were made. Breakages of the bonds are coloured according to their modes of failure and circled to represent a single seismic event. In the high-k-FZ-model, the fluid can easily migrate into the fault zone and lowers the normal stress and leads to shear failure of one contact which is registered as a single failure seismic event. Single seismic events can contain multiple bond breakages which means that those bond breakages take place within close time and space, due to the fact that one bond breakage triggers another near bond breakage.

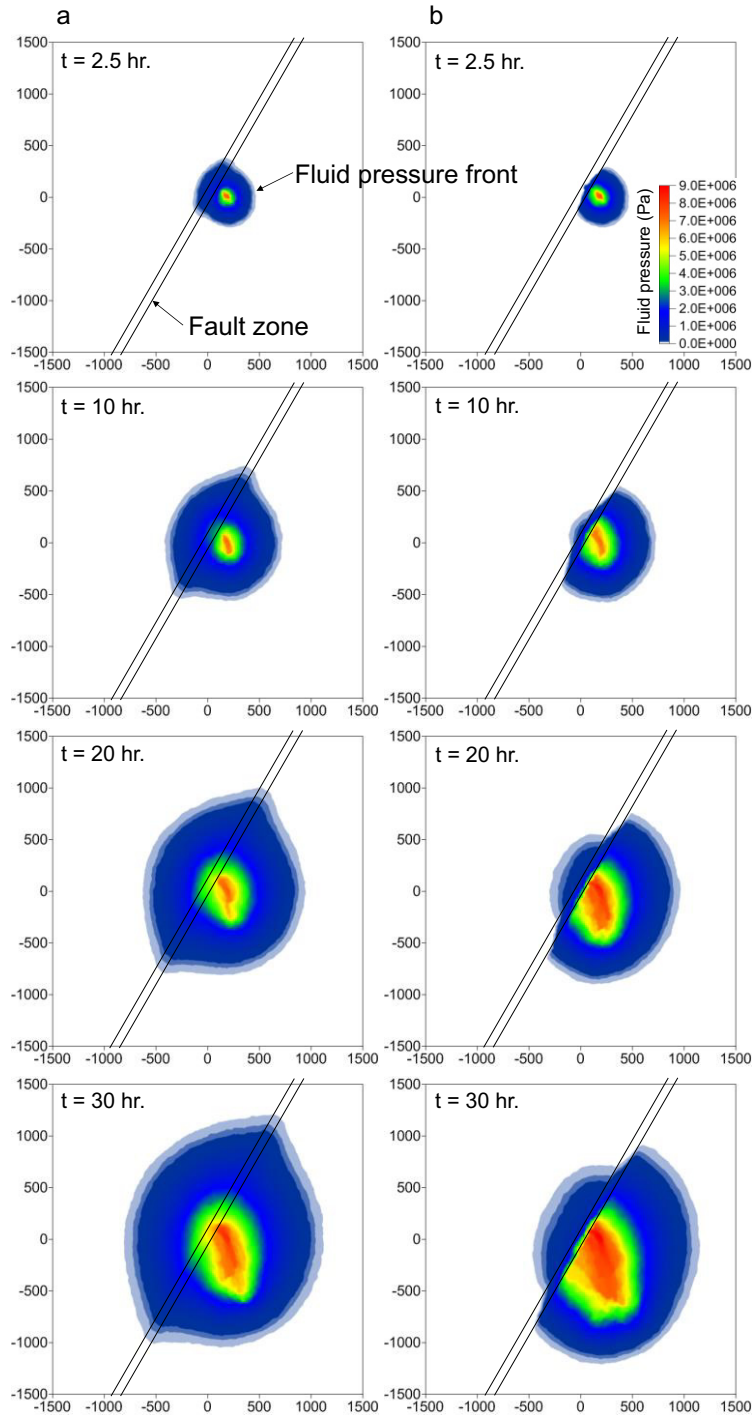


Fig. 6. Distribution of fluid pressure at different time during fluid injection in the (a) high-k-FZ and in (b) low-k-FZ-models.

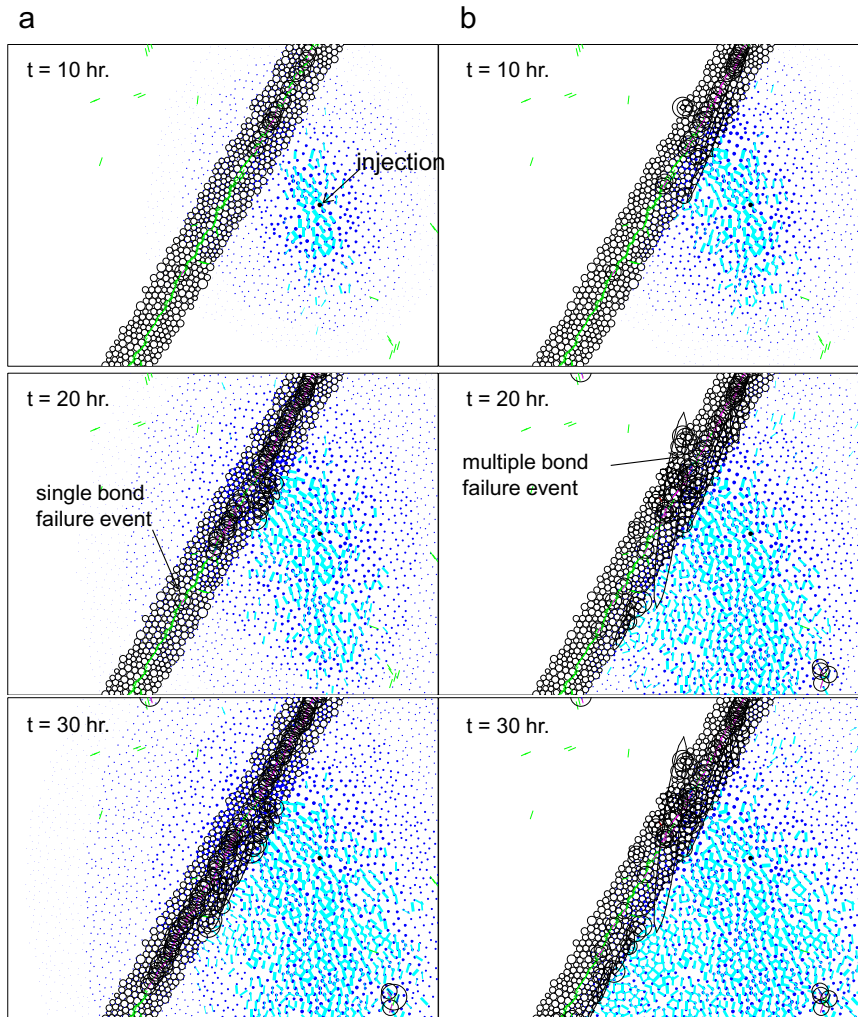


Fig. 7. Enlarged view of the model at the area of fluid injection in the (a) high-k-FZ and in (b) low-k-FZ-models at different times. Fluid pressure is indicated by the blue symbol of which the size represents the magnitude. Fluid flow is shown in cyan with the thickness of the symbol representing the volume of fluid flow at the time when the figure snapshots are made. Seismic events are represented by the black circles and ellipses for single failure events and multiple failure events, respectively.

Due to build-up of a large fluid pressure zone as shown in Figure 6, which leads to a higher and more near-critical state of stress, fluid migration at long-term reaches the fault core and leads to many seismic events associated with large stress drops. In the low-k-FZ-model, one induced failure triggers further seismic events and such domino-effect is more significant in the low-k-FZ-model and makes the magnitude-frequency distribution of the seismicity different from that in the high-k-FZ-model as shown in Figure 8. Gutenberg-Richter b-values are computed using the Maximum Likelihood Method [7] with the assumption that the moment completeness (M_c) is -0.6. The results show that the b-values are 1.9 and 0.9 in the high-k-FZ-model and in the low-k-FZ-model, respectively. This result, i.e. lower b-value under the higher stressed state, is consistent with several laboratory experiments [8].

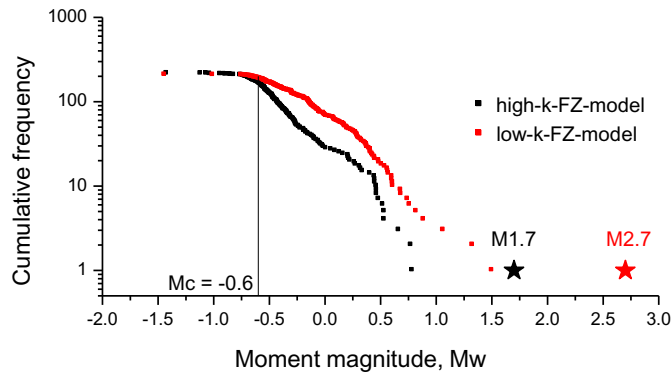


Fig. 8. Magnitude-frequency distribution of the modelled induced seismic events. Black and red stars are the modelled maximum magnitude associated with average slip of the fault core for the high and low-k-FZ-model, respectively.

4. Conclusions and outlook

We investigated numerically the evolution of seismic events induced by high-rate fluid injection near to a fault zone which is under a critical state by the initial in situ stress field. The model we present is able to simulate explicitly the hydro-mechanical and dynamically coupled processes that are responsible for occurrence of earthquakes induced by fluid injection. The resulting seismic response of the fault zone differs depending on the permeability contrast between the fault zone and the host rock mass. Magnitudes of induced seismicity evolving in the fault zone and magnitudes associated with slip of the fault core tend to be larger in case of fluid injection into a fault zone less permeable than the host rock mass due to large fluid pressure build-up on one side of the fault. The pressure then adds additional stress to the fault zone and leads to a stress state higher than the initial in situ stress field. Our results show that the magnitudes of fluid-injection-induced seismicity are generally larger in case of a fluid injection near to a less permeable fault system at a near-critical stress state than with permeable fault systems, and therefore the induced seismic hazard and risk may be larger. More investigations are under way which include: (1) spatially varied fluid saturation and regional stress field in the reservoir, (2) spatially varied fault zone permeability, (3) seismic events induced by fluid injection combined with fluid withdrawal, (4) effect of fault zone mechanical stiffness on the seismic reactivation, and (5) relating the mechanical (stiffness) and hydraulic (permeability) properties of the fault zones to their geological ages.

References

- [1] Majer EL, Baria R, Start M, Oates S, Bommer J, Smith B, Asanuma H. Induced seismicity associated with Enhanced Geothermal Systems. *Geothermics* 2007;36:185-222.
- [2] Keranen KM, Weingarten M, Abers GA, Bekins BA, Ge S. Sharp increase in central Oklahoma seismicity since 2008 induced by massive wastewater injection. *Science* 2014;345:448.
- [3] Hornbach MJ, DeShon HR, Ellsworth WL, Stump BW, Hayward C, Fröhlich C, Oldham HR, Olson JE, Magnani MB, Brokaw C, Luetgert JH. Causal factors for seismicity near Azle, Texas. *Nat. Commun.* 2015;6:6728.
- [4] Yoon JS, Zang A, Stephansson O. Numerical investigation on optimized stimulation of intact and naturally fractured deep geothermal reservoirs using hydro-mechanical coupled discrete particles joints model. *Geothermics* 2014;52:165-184.
- [5] Mas Ivars D, Pierce ME, Darcel C, Reyes-Montes J, Potyondy DO, Young RP, Cundall PA. The synthetic rock mass approach for jointed rock mass modelling. *Int. J. Rock Mech. & Min. Sci.* 2011;48:219-244.
- [6] Lay T, Wallace TC. *Modern Global Seismology*. Academic Press 1995, San Diego.
- [7] Bender B. Maximum likelihood estimation of b values for magnitude grouped data. *Bull. Seismol. Soc. Am.* 1983;73(3):831-851.
- [8] Amitrano D. Brittle-ductile transition and associated seismicity: Experimental and numerical studies and relationship with the b value. *J. Geophys. Res.* 2003;108(B1):2044.